Original Article

The effects of photobiomodulation therapy on inflammatory mediators, immune infiltration, and angiogenesis in a mouse model of rosacea

Shuwei Wu[1,2], Yaoxi Su[1,2], Lian Wang[1,2], Bensen Sun[1,2], Xian Jiang[1,2]

[1]Department of Dermatology, West China Hospital, Sichuan University, Chengdu, China; [2]Laboratory of Dermatology, Clinical Institute of Inflammation and Immunology, Frontiers Science Center for Disease-related Molecular Network, West China Hospital, Sichuan University, Chengdu, China

Contributions: (I) Conception and design: S Wu; (II) Administrative support: X Jiang; (III) Bioinformatics analyses: S Wu, Y Su, L Wang; (IV) Animal experiments: S Wu, B Sun; (V) Data analysis and interpretation: S Wu; (VI) Manuscript writing: All authors; (VII) Final approval of manuscript: All authors.

Correspondence to: Xian Jiang. No. 37 Guoxue Alley, Wuhou District, Chengdu 610041, China. Email: jennyxianj@163.com.

Background: Rosacea is a chronic skin disorder with increasing prevalence and challenging management. Photobiomodulation therapy (PBMT) may be a promising adjuvant treatment for rosacea.

Methods: This study investigated the efficacy of PBMT for the treatment of rosacea lesions in a well-established mouse model using a combination of wavelengths at 590 and 830 nm. Female BALB/c mice were randomized into three groups, namely, a negative control (NC) group, a model control (MC) group, and a PBMT group. Mice were injected with LL-37 or normal saline for construction of the model and NCs, respectively. Mice in the PBMT group were administered PBMT at wavelengths of 590 nm (25 mW) and 830 nm (50 mW). The severity of erythema, inflammatory cell counts, the expression of key inflammatory mediators, and the degree of angiogenesis and immune cell infiltration of the skin lesions were evaluated by hematoxylin and eosin (H&E) staining, immunohistochemistry, and immunofluorescence staining.

Results: PBMT significantly decreased the erythema scores and inflammatory cell infiltration of rosacea lesions in mice. Further studies revealed that PBMT downregulated the increased expression of inflammatory mediators (S100A9 and p65) and angiogenesis markers (CD31), and attenuated the dysregulation of immune cell infiltration [including neutrophils, regulatory T cells (Treg cells), γδ T cells, and macrophages] in mice with rosacea.

Conclusions: This investigation suggested that PBMT can improve the rosacea condition by regulating key inflammatory mediators and dysregulating immune infiltration and angiogenesis.

Keywords: Rosacea; photobiomodulation therapy (PBMT); angiogenesis; immune dysregulation; bioinformatics analyses

Submitted Jun 08, 2022. Accepted for publication Jul 14, 2022.
doi: 10.21037/atm-22-3204
View this article at: https://dx.doi.org/10.21037/atm-22-3204

Introduction

Rosacea is a chronic inflammatory disorder primarily affecting the centrofacial region, characterized by telangiectasia, transient or persistent erythema, inflammatory papules, and pustules (1). Rosacea affects approximately 5.5% of the global population and can cause disfigurement, emotional ramifications, and impairment of quality of life (2-6). Unfortunately, the pathophysiology of rosacea is not fully understood, and its management remains a challenge. Current evidence suggests that neurovascular dysregulation, as well as innate and adaptive immune dysregulation, play crucial roles in rosacea pathogenesis, and thus, these have

become predominant targets of multiple therapies (7).

Most rosacea patients experience repeated recurrences and exacerbations, and the management of rosacea remains taxing. Since a single factor or drug can hardly maintain the stable condition or reduce the recurrences, combination therapeutic strategies are often recommended, including topical agents, oral medication, injection therapy, and laser and light-based therapy. Among these treatments, laser and light-based therapy has been an important adjuvant regimen, especially for patients with long course, severe conditions, and multiple characteristics (8). Pulsed dye laser (PDL), potassium titanyl phosphate (KTP) laser, and intense pulsed light (IPL) are well-established therapies that can diminish erythema and remove telangiectasia in rosacea patients (9,10). Notably, although laser and light-based therapies can help improve the rosacea condition, the proper parameters should be set up with caution to prevent flares of rosacea and relevant side effects (9). Especially in patients with exacerbation rosacea, severe inflammation and skin barrier impairment often result in intolerance to the high-energy device, making the decision of the treatment timepoint rather difficult. Therefore, development of a safe and gentle light-based therapy is imperative to help achieve optimal outcomes for rosacea patients. Notably, photobiomodulation therapy (PBMT) is a kind of low-level laser (light) therapy, characterized by low energy and great safety profile.

PBMT, a light-based therapy with light emitting diodes (LEDs) as illuminants, has been applied to a variety of cutaneous disorders, including photoaging, vitiligo, psoriasis, acne, and skin scald (11). PBMT is characterized by low energy, low cost, easy operation, and is associated with a fairly excellent safety profile (12). It is also known for its anti-inflammatory, immunoregulatory, differentiation-promoting, and injury-repairing functions (13). PBMT has been shown to promote the proliferation of fibroblasts and stimulate keratinocyte migration and differentiation in cutaneous tissues (14-19). In addition, clinical observations have suggested that PBMT exerts an ideal therapeutic effect on sensitive skin by repairing the skin barrier and relieving erythema (20). PBMT can also regulate the activation of transient receptor potential vanilloid 1 (TRPV1), a crucial receptor implicated in the discomforts of rosacea (21,22). Notably, although PBMT has been accepted as an important adjuvant therapy for various skin disorders, its molecular mechanisms and targets have not been completely elucidated. Indeed, PBMT may be an effective therapeutic treatment for rosacea due to its anti-inflammatory function. Therefore, the efficacy of PBMT on rosacea and the underlying mechanisms warrant further investigation.

Herein, bioinformatics analyses were conducted to identify the crucial genes, pathways, and immune cells implicated in the pathophysiology of rosacea. The effects of PBMT at specific wavelengths and energy on rosacea were evaluated through *in vivo* studies. Finally, the underlying mechanisms were investigating by examining the effects of PBMT on the expression of crucial genes and immune cells using bioinformatics analyses. Specifically, we not only focused on the inflammatory mediators in the mechanism, but also the immune infiltration and angiogenesis, which are crucial part of rosacea pathogenesis. This study aimed to provide preliminary evidence for the therapeutic potential of PBMT on rosacea. We present the following article in accordance with the ARRIVE reporting checklist (available at https://atm.amegroups.com/article/view/10.21037/atm-22-3204/rc).

Methods

Identification of differentially expressed genes (DEGs) in patients with rosacea

The gene expression data of rosacea tissues and healthy tissues were acquired from the Gene Expression Omnibus (GEO) of the National Center for Biotechnology Information (NCBI) (http://www.ncbi.nlm.nih.gov/geo). All the research involving GEO database was conducted in accordance with the Declaration of Helsinki (as revised in 2013). The GSE65914 dataset, composed of 38 rosacea tissues and 20 healthy tissues, was examined in this study. The R software version 4.1.1 was used to analyze and visualize the expression profile data. The gene expression data were first processed through calibration and standardization. The DEGs were identified with a threshold of $|\log2 \text{(fold change)}| > 1$ and corrected P value [false discovery rate (FDR)] <0.05. Visualization of the DEGs was performed with hierarchic clustering heatmaps and volcano maps.

Gene Ontology (GO), Kyoto Encyclopedia of Genes and Genomes (KEGG), and gene set enrichment analyses

GO analysis was conducted using the "clusterProfiler" package in R software to identify the functions of the candidate DEGs. Three different phenotypes of rosacea, including erythematotelangiectatic rosacea (ETR), papulopustular rosacea (PPR), and phymatous rosacea

(PhR), were distinguished for analysis. Enrichment of the DEGs in different signaling pathways was investigated using the KEGG analysis and gene set enrichment analysis (GSEA). A P value <0.05 was set as the cut-off value. Bubble plots were generated to visualize the results of the GO and KEGG analyses by the "ggplot2" package in R software.

Immune cell infiltration analyses

Single-sample gene set enrichment analysis (ssGSEA) and the CIBERSORT algorithm were used to analyze the abundances and compositions of immune cell infiltrations in rosacea tissues. ssGSEA was conducted to evaluate the degree of infiltration of different immune cell types, immune-related functions, and immune-related pathways in the gene expression profile. The "gsva" package in R software was used to calculate the enrichment scores (ES) of the marker genes in the expression data. The expression matrix of 22 kinds of immune cells in CIBERSORT (http://cibersort.stanford.edu/) was downloaded. CIBERSORT analysis was performed to calculate the composition ratio of 22 immune cells in rosacea and healthy tissues. Permutation analysis was subsequently performed. A P value <0.05 was considered statistically significant.

Reagents and equipment

The 37-amino-acid peptide (LL-37 peptide) was purchased from InvivoGen, San Diego, CA. The LL-37 powder was dissolved in normal saline to generate a LL-37 solution with a concentration of 320 μM/L, and stored at 4 ℃. 4',6-diamidino-2-phenylindole (DAPI) was purchased from Abcam (Cambridge, UK). 3,3'-diaminobenzidine (DAB) was purchased from ZSGB-BIO Technology, Beijing, China. The optical microscope and histological slice scanner were obtained from Olympus, Tokyo, Japan. The NIS-Elements AR was purchased from Nikon, Japan. The laser scanning confocal microscope (Leica s-STELLARIS) was purchased from Leica, Germany.

Animal experiments

A protocol was prepared before the study without registration. Eighteen female BALB/c mice (6 weeks old and weighing 19.89±2.01 g) were obtained from Chengdu Dossy Experimental Animals Co., Ltd. (Chengdu, China). All animal experiments performed in this study were approved by the Animal Ethics Committee of West China Hospital (Approval No. 20211133 A), in compliance with institutional guidelines for the care and use of animals. The mice were given free access to standard food and water. The animals were specific pathogen free (SPF) mice with normal immune function and without any genetic modifications. The mice were acclimated to the experimental conditions for one week before experimentation. The mice were randomized into 3 groups of 6 mice each, namely, a negative control (NC) group, a model control (MC) group, and a PBMT group. The randomization was generated using a table of random numbers for random grouping. The dorsal skin of each mouse was gently shaved 24 hours prior to experimentation.

The rosacea-like skin model of mice was induced by administration of the LL-37 peptide, as previously described (23-32). To induce rosacea-like skin lesions, intradermal injections of 50 μL of LL-37 were delivered 4 times every 12 hours to the shaved dorsal skin of the mice in the MC and PBMT groups. Accordingly, intradermal injection of normal saline was applied at the same dose and frequency to the mice in the NC group. Twenty-four hours after the last injection, the skin lesions of all the mice were photographed and evaluated by redness scores, as previously described (29). The redness scores were evaluated by a researcher who was completely blinded to the study design. The mice were then sacrificed by deep anesthesia. The full-thickness dorsal skin tissues were biopsied for subsequent hematoxylin and eosin (H&E staining), immunohistochemistry, and immunofluorescence staining.

PBMT protocol

The parameters of the PBMT were as follows: (I) the treatment light was a combination of 590 and 830 nm wavelengths; and (II) the energy was 25 mW for the 590 nm wavelength and 50 mW for the 830 nm wavelength. The light source was set 10 cm from the mouse skin. Half an hour before the third and fourth injections, as well as 12 hours after the fourth injection, the dorsal skin of the mice in the PBMT group was treated with PBMT for 5 minutes each time. The total irradiation time was 15 minutes for every mouse throughout the whole treatment (5 minutes per day, 3 days). The parameters are summarized in *Table 1*.

Histological analysis

The skin tissues of mice were fixed in 4% paraformaldehyde and embedded in paraffin. H&E staining was performed

Table 1 Parameters of the photobiomodulation therapy protocol

Wavelength (nm)	Power (mW)	Distance (cm)	Total time (minutes)	Total energy (J)
590	25	10	15	22.5
830	50	10	15	45

on prepared sections and visualized under an optical microscope at ×10 and ×20 magnification. Six random fields of view were captured and the number of dermis-infiltrating inflammatory cells in each field was calculated using Image-Pro Plus 6.0 software. The counting of infiltrating inflammatory cells was conducted by a researcher who was completely blinded to the study.

Immunohistochemistry

The expression of p65 and S100A9 in mouse skin tissues was detected by immunohistochemistry following the standard protocol. Sections were rehydrated and incubated with primary antibodies against NF-κB/p65 (ab16502, Abcam, UK) and S100A9 (ab92507, Abcam, UK) overnight at 4 ℃. The sections were then incubated with goat anti-rabbit secondary antibody [Goat AntiRabbit IgG H&L (HRP), ab205718, Abcam, UK] for 1 hour at room temperature. Subsequently, sections were washed and counterstained with DAB/hematoxylin (ZSGB-BIO Technology, Beijing, China). Images were captured using NIS-Elements AR (Nikon, Japan) and analyzed by Image J software with IHC Profiler Plugin.

Immunofluorescence

The expression of CD31, as well as the infiltration of neutrophils, regulatory T cells (Treg cells), γδ T cells, and macrophages were detected by immunofluorescence staining. Sections were treated with citric acid (ZSGB-BIO Technology, Beijing, China) for antigen retrieval and incubated with primary antibodies overnight at 4 ℃. Tissues were then incubated with a secondary antibody (Goat Anti-Rabbit IgG H&L, Alexa Fluor® 488) for 40 minutes at room temperature. Images were captured using a Leica s-STELLARIS (Leica, Germany) microscope and analyzed with Image J analysis software. The primary antibodies against CD31 (ab182981, Abcam, UK), CD66b (ab197678, Abcam, UK), GR-1 (68590, Cell Signaling Technology, Danvers, MA, USA), CD4 (ab183685, Abcam, UK), Foxp3 (ab215206, Abcam, UK), CD3 (ab16669, Abcam, UK), TCRγδ (ab25209, Abcam, UK), CD80 (ab254579, Abcam, UK), and F4/80 (ab6640, Abcam, UK) were used in this study. Specifically, DAPI was used to stain the cellular nuclei; CD31 was used to mark vascular endothelial cells; CD66b and GR-1 were used to mark neutrophils; CD4 and Foxp3 were used to mark Treg cells; CD3 and TCRγδ were used to mark γδ T cells; and CD80 and F4/80 were used to mark macrophages (33).

Statistical analysis

All data were recorded with Microsoft Excel 2019 and presented as the means ± standard error of the mean (SEM). Data were analyzed with IBM SPSS Statistics 25. The comparison of different groups was performed using independent *t* tests, one-way analysis of variance (ANOVA), SNK tests, and Dunnett *t*-tests. All tests were two-sided tests, and a P value <0.05 was considered statistically significant.

Results

The DEGs in rosacea and their functional annotation

The GEO dataset (GSE65914) included in this study was composed of 38 cases of rosacea lesions (including 14 cases of ETR, 12 cases of PPR, and 12 cases of PhR) and 20 cases of healthy controls. A total of 3,016 DEGs between rosacea tissues and healthy tissues were identified, which were visualized using a volcano plot (*Figure 1A*). The top-ranked differentially expressed messenger RNAs (mRNAs) and long noncoding RNAs (lncRNAs) are shown in the hierarchical clustering heatmap (*Figure 1B*). Notably, S100A9 was found to be most upregulated in rosacea patients (*Figure 1B*). The results of GO analysis suggested that the DEGs of rosacea were mainly involved in leukocyte migration, T-cell activation, regulation of vasculature development, regulation of angiogenesis, and neutrophil chemotaxis (*Figure 1C*). KEGG analysis revealed that the DEGs were mainly enriched in pathways including cytokine-cytokine receptor interaction, chemokine signaling pathway, and *Staphylococcus aureus* infection (*Figure 1D*). The GSEA results showed that the pathways with the top 2 ES of

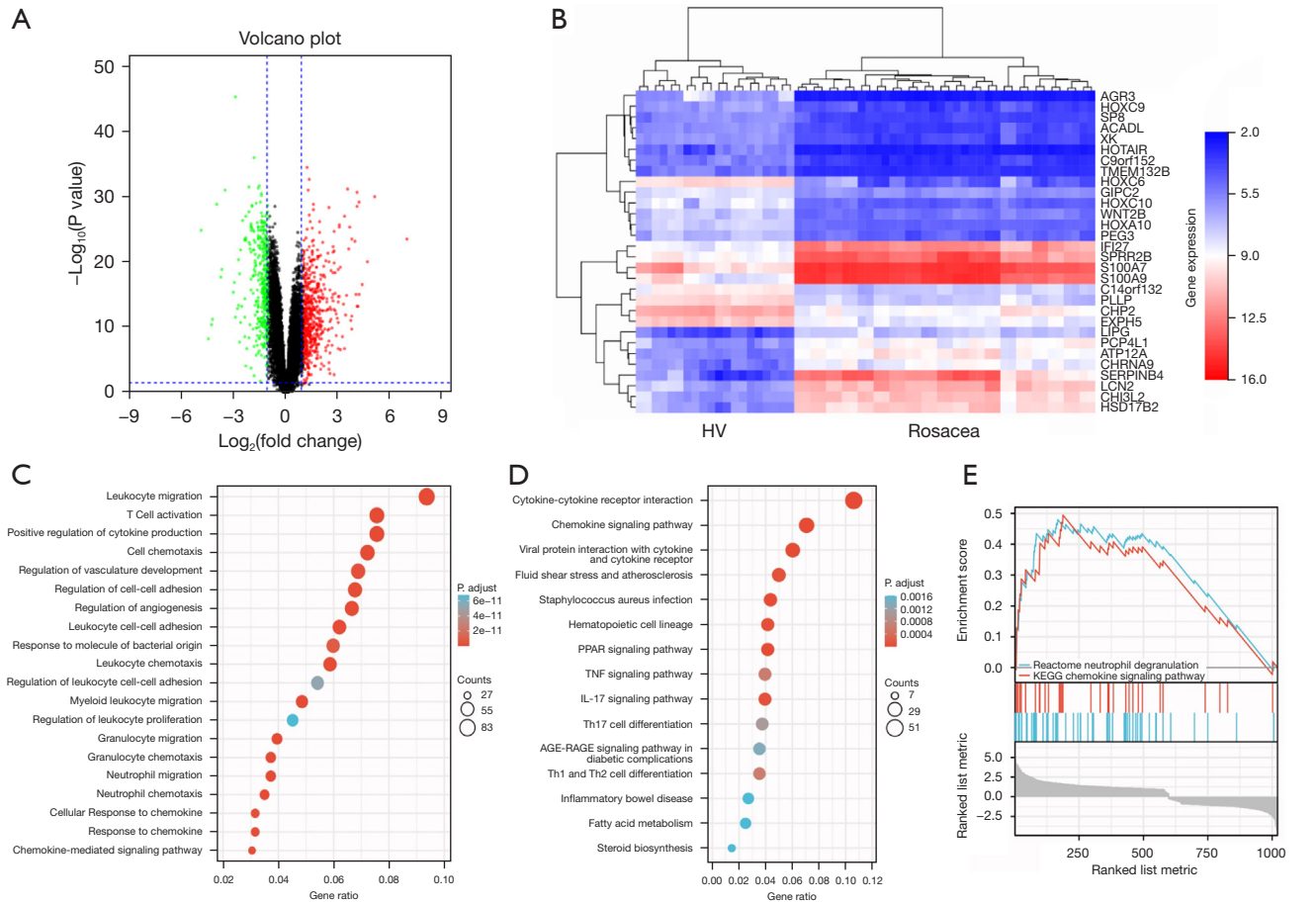

Figure 1 Identification and functional annotation of the differentially expressed genes between rosacea tissues and healthy controls. (A) A volcano plot showing the upregulated DEGs (red dots) and downregulated DEGs (green dots) of rosacea tissues compared with healthy controls. (B) A hierarchical clustering heatmap showing the predominant differentially expressed mRNAs and lncRNAs of rosacea tissues compared with healthy controls. The expression of S100A9 was significantly upregulated. (C) A bubble plot showing the enrichment of the candidate DEGs by GO analysis. (D) A bubble plot showing the enrichment of the candidate DEGs by KEGG analysis. (E) The enrichment score ranking of the DEGs by GSEA. The pathways with the highest enrichment scores were neutrophil degranulation and the chemokine signaling pathway. HV, healthy volunteers; PPAR, peroxisome proliferator activated receptors; TNF, tumor necrosis factor; IL-17, interleukin-17; Th17, T helper cell 17; Th1 cell, T helper cell 1; Th2 cell, T helper cell 2; DEG, differentially expressed genes; mRNA, messenger RNA; lncRNA, long non-coding RNA; GO, Gene Ontology; KEGG, Kyoto Encyclopedia of Genes and Genomes; GSEA, Gene Set Enrichment Analysis.

rosacea were neutrophil degranulation and the chemokine signaling pathway (*Figure 1E*). Taken together, these results highlight the central role of immune activation, inflammatory pathways, and angiogenesis in the pathophysiology of rosacea.

The immune infiltration of rosacea

A variety of immune cells were found to differentially infiltrate rosacea tissues compared with healthy controls according to ssGSEA (*Figure 2A*). The differential infiltration of 22 types of immune cells between rosacea tissues and healthy controls, based on different subtypes (ETR, PPR, PhR), was analyzed by CIBERSORT. Notably, there were 4 types of immune cells that were differentially infiltrated in all 3 subtypes of rosacea, namely activated $CD4^+$ memory T cells, γδ T cells, M1 macrophages, and Treg cells (*Figure 2B*). Specifically, the infiltration

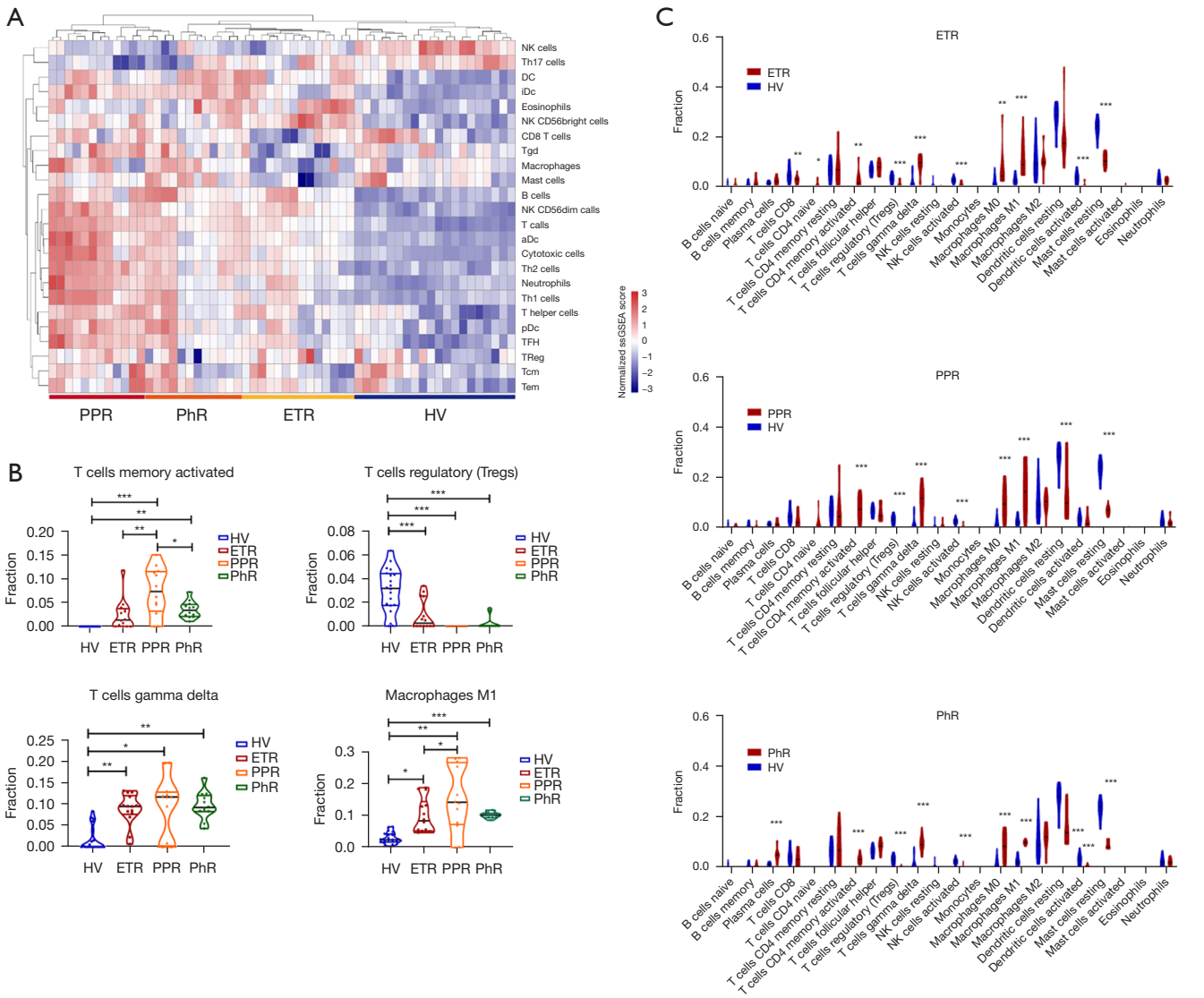

Figure 2 Immune infiltration analysis of rosacea lesions. (A) A hierarchical clustering heatmap showing the differential infiltration of immune cells between rosacea patients (ETR, PPR, and PhR) and healthy controls. (B) The differential infiltration of activated CD4$^+$ memory T cells, γδ T cells, M1 macrophages, and Treg cells. In three different subtypes of rosacea, activated CD4$^+$ memory T cells, γδ T cells, and M1 macrophages were enriched in rosacea, whereas Treg cells were decreased. *, P<0.05; **, P<0.01; ***, P<0.001. (C) The differential infiltration of 22 types of immune cells in 3 different subtypes of rosacea. *, P<0.05; **, P<0.01; ***, P<0.001. PPR, papulopustular rosacea; PhR, phymatous rosacea; ETR, erythematotelangiectatic rosacea; HV, healthy volunteers; NK cells, natural killer cells; Th17 cells, T helper cells 17; DC, dendritic cells; iDc, immature dendritic cells; Tgd, γδ T cells; aDc, activated dendritic cells; Th1 cell, T helper cells 1; Th2 cell, T helper cells 2; pDc, plasmacytoid dendritic cells; TFH, follicular helper T cells; TReg, regulatory T cells; Tcm, central memory T cells; Tem, effective memory T cells.

of activated CD4$^+$ memory T cells, γδ T cells, and M1 macrophages was significantly increased in rosacea, whereas the infiltration of Treg cells was significantly decreased compared with healthy controls. Apart from that, the immune infiltration of different subtypes of rosacea (ETR, PPR and PhR) was quite different. For instance, initial CD4$^+$ T cells were only enriched in the ETR; dendritic cells were only enriched in the PPR; and plasma cells were only

enriched in the PhR (*Figure 2C*).

PBMT alleviated the inflammatory response and angiogenesis of rosacea-like skin in mice

Intradermal injection of LL-37 in mice resulted in rosacea-like phenotypes, including erythema and inflammatory cell infiltration (*Figure 3A,3B*). Administration of PBMT significantly reduced the redness scores of the rosacea-like lesions (*Figure 3C*). Compared with the MC group, the inflammatory cell counts of the PBMT group were dramatically decreased (*Figure 3B,3D*). Histological analysis revealed that there was a disordered arrangement of collagen fibers in the MC group compared with the NC group. Notably, the dermal collagen fibers appeared to be thickened and arranged more orderly in rosacea-like lesions after receiving PBMT (*Figure 3B*). As shown in previous studies and our informatics analyses, p65 and S100A9 are two key inflammatory mediators of rosacea (31-36). The expression levels of S100A9 and p65 were significantly upregulated in rosacea-like mouse skin compared to NC skin, and this was significantly repressed after administration of PBMT (*Figure 3E*). CD31 is a key marker of vascular endothelial cells, and is often used to identify and quantify neovascularization. The expression of CD31 was reduced after PBMT in rosacea-like skin (*Figure 3F*). These results demonstrated that PBMT attenuated the severity of erythema, the inflammatory response, and angiogenesis in rosacea-like mouse skin.

PBMT attenuated the dysregulation of immune cell infiltration of rosacea-like skin in mice

The bioinformatics analyses identified 4 types of differentially infiltrated immune cells in 3 subtypes of rosacea, namely activated $CD4^+$ memory T cells, γδ T cells, M1 macrophages, and Treg cells. The infiltration of these immune cells was evaluated using the *in vivo* model as an important indicator for immune dysregulation. Based on previous studies (33,37-39), CD66B and GR-1 were used to mark neutrophils (*Figure 4A*), CD4 and Foxp3 were used to mark Treg cells (*Figure 4B*), CD3 and TCRγδ were used to mark γδ T cells (*Figure 5A*), and CD80 and F4/80 were used to mark macrophages (*Figure 5B*). The results showed that the infiltration of neutrophils, γδ T cells, and macrophages was increased in rosacea-like skin compared with the NC group, while the infiltration of Treg cells was decreased (*Figures 4,5*). Compared with the MC group, the infiltration of neutrophils, γδ T cells, and macrophages was decreased in the PBMT group, while the infiltration of Treg cells was increased (*Figures 4,5*). The infiltration of neutrophils, Treg cells, γδ T cells, and macrophages in the PBMT group was similar to that observed in the NC group. Collectively, these results suggested that PBMT suppressed immune dysregulation by reducing the infiltration of neutrophils, γδ T cells, macrophages, and increasing the infiltration of Treg cells in rosacea-like mouse skin.

Discussion

Rosacea is a chronic inflammatory disorder characterized by recurrent remission and exacerbation. Despite a variety of therapeutic options, the management of rosacea remains a challenge. Laser and light-based therapies are important adjuvant treatments for rosacea patients, and diminish the associated erythema and telangiectasia (12). Nevertheless, many of these therapies have high energy and may trigger the flares of rosacea. PBMT, characterized by low energy, as well as anti-inflammatory and immunoregulatory properties, may be a better choice for rosacea patients with an impaired skin barrier and severe inflammation. The present study demonstrated through an *in vivo* model that PBMT attenuated the severity of erythema, inflammatory response, immune dysregulation, and angiogenesis in rosacea-like mouse skin. The skin is a multi-layer organ, composed of various kinds of cells. There are multiple interactions and crosstalk among different layers and cells. Therefore, an *in vivo* model may be more suitable to simulate the human skin.

Although the pathogenesis and pathophysiology of rosacea are not fully understood, innate and adaptive immune dysregulation and neurovascular dysregulation are known to play crucial roles in rosacea pathogenesis (7). The results from our bioinformatics analyses support the current understanding and showed that the DEGs of rosacea were predominantly enriched in pathways related to infections, inflammatory responses, and immunological and vascular dysregulation. As a key inflammatory mediator, S100A9 was found to be most upregulated in rosacea lesions. In addition, the infiltration of activated $CD4^+$ memory T cells, Treg cells, and M1 macrophages in the three subtypes of rosacea were all increased, while the infiltration of γδ T cells was decreased. These results indicated that the noted genes, pathways, and immune cells may be closely related to the pathophysiology of rosacea. To validate this hypothesis, the expression of these genes and immune cell infiltration were

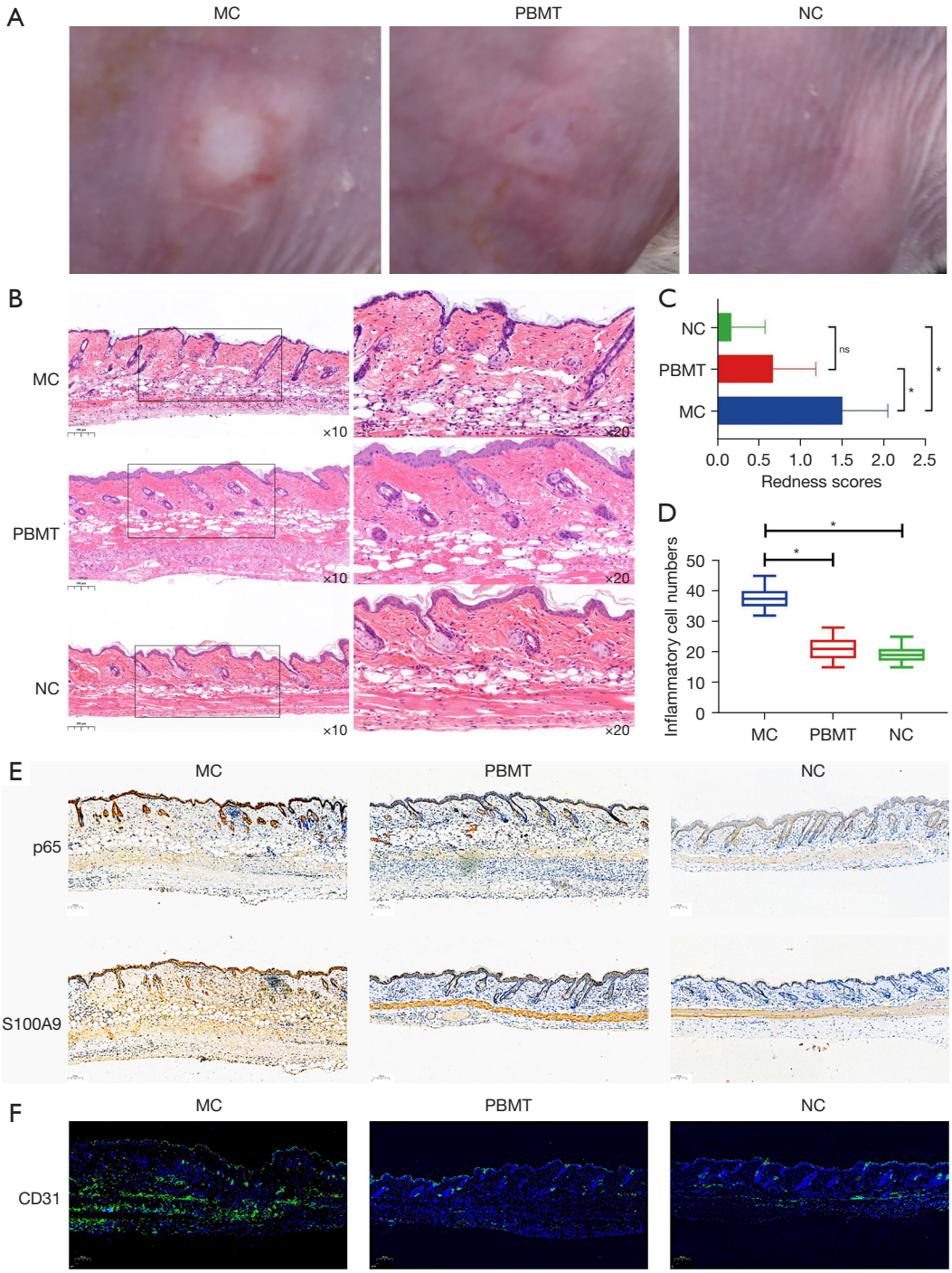

Figure 3 PBMT attenuated the severity of erythema, the inflammatory response, and angiogenesis in rosacea-like mouse skin in BALB/c mice. (A) Photographs of the dorsal skin lesions from the MC, PBMT, and NC groups. (B) H&E staining of skin lesions from the MC, PBMT, and NC groups. Scale bar =100 μm. (C) The redness scores of the skin lesions in the MC, PBMT, and NC groups (n=18, *, P<0.05; ns, not significant). (D) The inflammatory cell counts of the MC, PBMT, and NC groups based on H&E staining (n=18, *, P<0.05). (E) The expression of p65 and S100A9 in skin lesions from the MC, PBMT, and NC groups by immunohistochemistry. Scale bar =100 μm. (F) The expression of CD31 in the skin tissue from the MC, PBMT, and NC groups by immunofluorescence staining. Scale bar =100 μm. MC, model control; NC, negative control; PBMT, photobiomodulation therapy; H&E, hematoxylin and eosin.

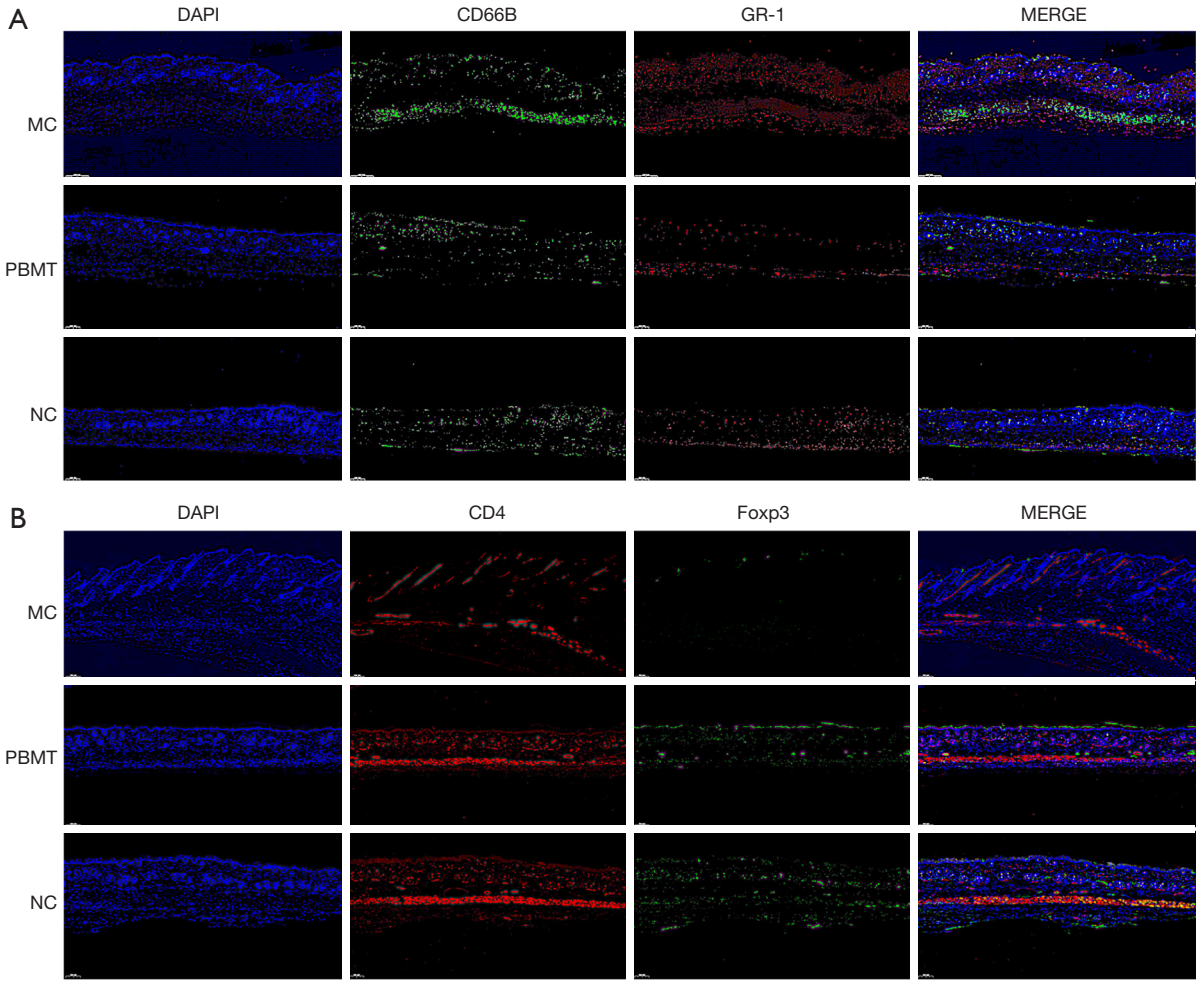

Figure 4 The infiltration status of neutrophils and γδ T cells in mouse skin tissues from the NC, MC and PBMT groups, as observed by immunofluorescence staining. (A) The infiltration status of neutrophils marked by CD66B (green fluorescence) and GR-1 (red fluorescence). Scale bar =100 μm. (B) The infiltration status of Treg cells as determined by CD4 staining (red fluorescence) and Foxp3 staining (green fluorescence). Scale bar =100 μm. MC, model control; PBMT, photobiomodulation therapy; NC, negative control; Treg, regulatory T cell.

evaluated using an *in vivo* model. In agreement with the bioinformatics results, parallel dysregulation was detected in the *in vivo* model, namely, significantly upregulated S100A9 and similar infiltration of the four types of immune cells. This finding further confirmed the suitability of this mouse model for examining the effects of rosacea in humans. Furthermore, this report supports the crucial roles of these genes and immune cells in rosacea pathophysiology.

In the present study, PBMT with wavelengths of 590 and 830 nm ameliorated rosacea-like skin by alleviating the severity of erythema and decreasing inflammatory cell infiltration. Further investigation demonstrated that PBMT significantly downregulated the expression of two key inflammatory mediators (p65 and S100A9), decreased the expression of CD31, and attenuated the dysregulated infiltration of the four types of immune cells (namely, neutrophils, γδ T cells, macrophages, and Treg cells) in rosacea-like skin. Of note, the S100A9 protein (a member of the S100 protein family) is crucial in neutrophil and leukocyte recruitment, as well as neutrophil-related fibronectin adhesion (34). It was demonstrated that the NEAT1/miR-196a-5p/S100A9 axis may have played an important role in the dynamics underlying inflammatory responses of rosacea (34). Therefore, it may contribute to the dysregulated infiltration of immune cells in the rosacea-like mouse skin. The p65 protein is a crucial molecule

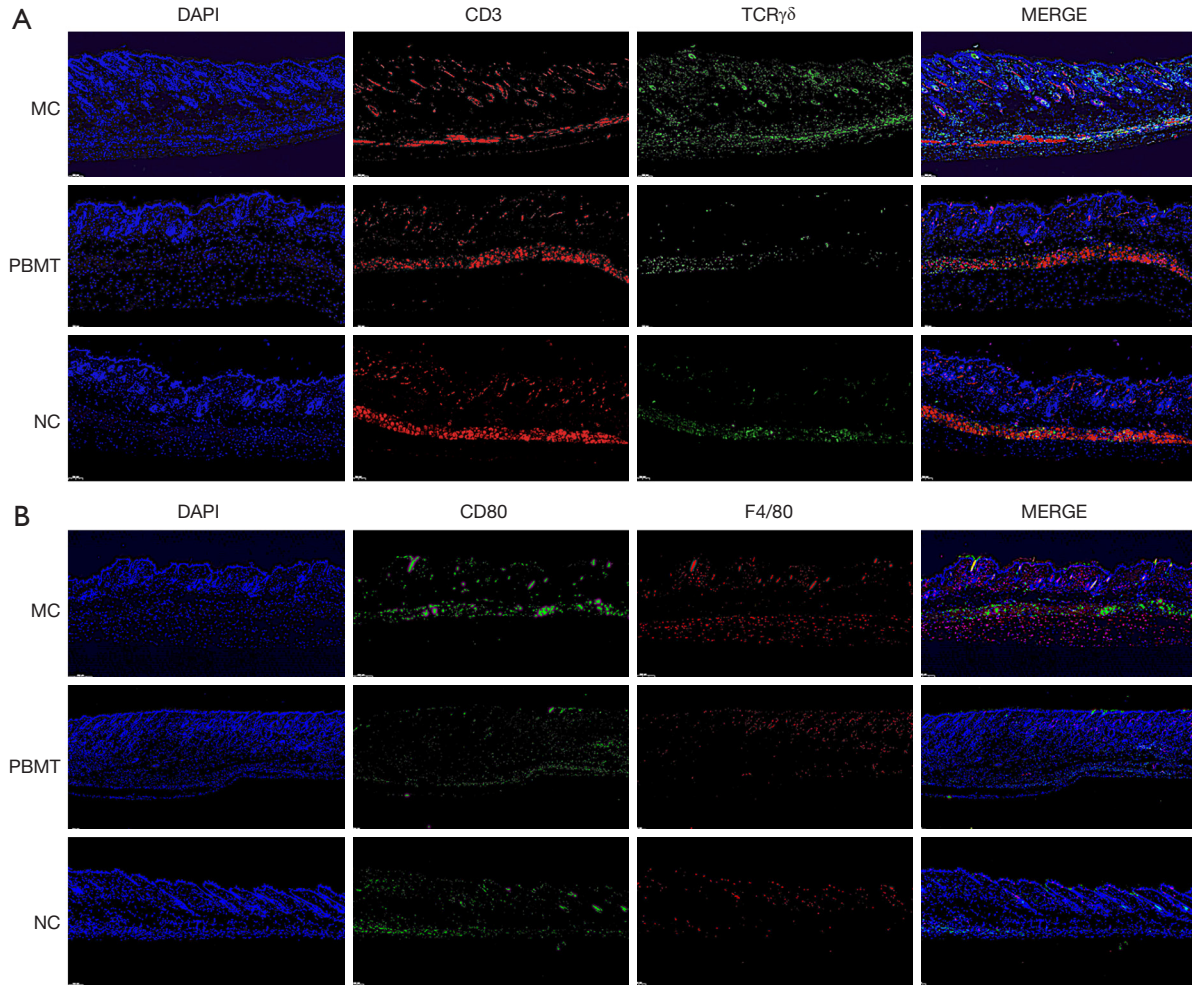

Figure 5 The infiltration status of macrophages and Treg cells in mouse skin tissues from the NC, MC and PBMT groups, as observed by immunofluorescence staining. (A) The infiltration status of γδ T cells marked by CD3 (red fluorescence) and TCRγδ (green fluorescence). Scale bar =100 μm. (B) The infiltration status of macrophages as determined by CD80 (green fluorescence) and F4/80 (red fluorescence) staining. Scale bar =100 μm. MC, model control; PBMT, photobiomodulation therapy; NC, negative control; Treg, regulatory T cell.

in the activation of the NF-κB pathway (35), which was significantly downregulated by PBMT in this study. A previous study also demonstrated that PBMT can regulate histone acetylation and NF-κB expression (19). In addition, S100A8/A9 can promote the NF-κB pathway by activating toll-like receptor 4 (TLR4) through the MyD88-dependent pathway, which is downregulated by PBMT in rosacea-like skin (36). These findings indicated that PBMT may alleviate inflammation by inhibiting the NF-κB pathway and the downstream inflammatory response (35). The results of the present report are in accordance with these previous studies. The present study also demonstrated that PBMT attenuated the abnormal infiltration of crucial immune cells implicated in rosacea pathogenesis. Taken together, PBMT may suppress the inflammatory response of rosacea by inhibiting immune cell recruitment and crucial inflammatory pathways. Furthermore, PBMT inhibited angiogenesis in rosacea-like mouse skin. Although PBMT has been reported to have multiple benefits, there is limited evidence supporting the anti-angiogenesis effect of PBMT. Herein, the expression of CD31, a key marker for angiogenesis, was significantly downregulated by PBMT in rosacea-like lesions. However, the underlying mechanisms of the anti-angiogenic function of PBMT warrant further investigation. Indeed, the suppression of angiogenesis may be partly attributed to its inhibition of the inflammatory

response, considering the neuroinflammatory characteristic of rosacea.

Apart from its anti-inflammatory function, previous studies have revealed that PBMT can regulate the activation of TRPV1, thereby relieving the discomfort, including burning, stinging, and itching, associated with rosacea (21,22). Moreover, it has been suggested that PBMT can promote the growth and proliferation of fibroblasts (14-18), and stimulate keratinocyte migration and differentiation (19). The histological studies herein demonstrated that the dermal collagen fibers were thickened and arranged more orderly in rosacea-like lesions after PBMT. Therefore, PBMT may improve rosacea lesions by mediating epidermal regeneration, repairing the skin barrier, and increasing dermal collagens. Notably, a previous study demonstrated that LED at 630 and 940 nm downregulated the expression of key inflammatory mediators in rosacea, as well as protease activity in keratinocytes and rosacea-like mouse skin (28). The present study further supported the conclusion that PBMT can alleviate the inflammatory response of rosacea. PBMT downregulated the expression of S100A9 and p65, which suggested that PBMT might suppress the inflammatory response by inhibiting the NF-κB pathway. Moreover, the abnormal infiltration of immune cells was alleviated by PBMT, indicating that it may alleviate inflammation by inhibiting leukocyte recruitment and immune infiltration. Furthermore, PBMT may suppress angiogenesis, which may also help improve rosacea. Taken together, this study demonstrated that PBMT can alleviate the inflammation and erythema of rosacea-like skin, and may have therapeutic potential in the management of rosacea. However, the current evidence is limited to *in vivo* and *in vitro* studies, and further high-quality clinical investigations are warranted to further elucidate the effects of PBMT on rosacea.

There were several limitations to this study. First, a parameter array was not set up in this study. While the parameters of PBMT were fixed, the optimal parameters for rosacea remain to be elucidated. Second, clinical evaluation was not conducted in this study and the efficacy of PBMT in humans requires further investigation. Finally, although the method for inducing rosacea-like mouse skin has been reported in previous studies, the current model was not able to completely simulate the rosacea lesions in humans. In summary, the present study may provide candidate DEGs and for the subsequent investigation or therapy for rosacea. The dysregulated infiltration of the four immune cell, demonstrating that they may play an important role in the rosacea pathogenesis, which may become potential targets for the rosacea therapy (especially immune therapy). More importantly, the present study provided preliminary evidence for the therapeutic effects of PBMT on rosacea. In particular, PBMT inhibited the immune recruitment and crucial inflammatory pathways of rosacea, and may exert anti-angiogenic and barrier-repairing functions, which may improve the condition of patients with rosacea.

Acknowledgments

The authors would like to pay tribute to the patients and investigators who participated in the GEO and provided data selflessly.

Funding: This work was supported by the National Natural Science Foundation of China (Nos. 81872535 and 82073473); the 1·3·5 Project for Disciplines of Excellence, West China Hospital, Sichuan University (No. ZYJC21036); and the Clinical Research Innovation Project, West China Hospital, Sichuan University (No. 2019HXCX10).

Footnote

Reporting Checklist: The authors have completed the ARRIVE reporting checklist. Available at https://atm.amegroups.com/article/view/10.21037/atm-22-3204/rc

Data Sharing Statement: Available at https://atm.amegroups.com/article/view/10.21037/atm-22-3204/dss

Conflicts of Interest: All authors have completed the ICMJE uniform disclosure form (available at https://atm.amegroups.com/article/view/10.21037/atm-22-3204/coif). The authors have no conflicts of interest to declare.

Ethical Statement: The authors are accountable for all aspects of the work in ensuring that questions related to the accuracy or integrity of any part of the work are appropriately investigated and resolved. All the research involving GEO database was conducted in accordance with the Declaration of Helsinki (as revised in 2013). All animal experiments performed in this study were approved by the Animal Ethics Committee of West China Hospital (Approval No. 20211133 A), in compliance with institutional guidelines for the care and use of animals.

Open Access Statement: This is an Open Access article

References

1. Zhang H, Tang K, Wang Y, et al. Rosacea Treatment: Review and Update. Dermatol Ther (Heidelb) 2021;11:13-24.
2. Oussedik E, Bourcier M, Tan J. Psychosocial Burden and Other Impacts of Rosacea on Patients' Quality of Life. Dermatol Clin 2018;36:103-13.
3. Marson JW, Baldwin HE. Rosacea: a wholistic review and update from pathogenesis to diagnosis and therapy. Int J Dermatol 2020;59:e175-82.
4. Wu Y, Fu C, Zhang W, et al. The dermatology life quality index (DLQI) and the hospital anxiety and depression (HADS) in Chinese rosacea patients. Psychol Health Med 2018;23:369-74.
5. Cardwell LA, Nyckowski T, Uwakwe LN, et al. Coping Mechanisms and Resources for Patients Suffering from Rosacea. Dermatol Clin 2018;36:171-4.
6. Gether L, Overgaard LK, Egeberg A, et al. Incidence and prevalence of rosacea: a systematic review and meta-analysis. Br J Dermatol 2018;179:282-9.
7. Ahn CS, Huang WW. Rosacea Pathogenesis. Dermatol Clin 2018;36:81-6.
8. Husein-ElAhmed H, Steinhoff M. Laser and light-based therapies in the management of rosacea: an updated systematic review. Lasers Med Sci 2021;36:1151-60.
9. Shim TN, Abdullah A. The effect of pulsed dye laser on the dermatology life quality index in erythematotelangiectatic rosacea patients: an assessment. J Clin Aesthet Dermatol 2013;6:30-2.
10. van Zuuren EJ, Arents BWM, van der Linden MMD, et al. Rosacea: New Concepts in Classification and Treatment. Am J Clin Dermatol 2021;22:457-65.
11. Barolet D. Light-emitting diodes (LEDs) in dermatology. Semin Cutan Med Surg 2008;27:227-38.
12. Avci P, Gupta A, Sadasivam M, et al. Low-level laser (light) therapy (LLLT) in skin: stimulating, healing, restoring. Semin Cutan Med Surg 2013;32:41-52.
13. Glass GE. Photobiomodulation: The Clinical Applications of Low-Level Light Therapy. Aesthet Surg J 2021;41:723-38.
14. Carrinho PM, Renno AC, Koeke P, et al. Comparative study using 685-nm and 830-nm lasers in the tissue repair of tenotomized tendons in the mouse. Photomed Laser Surg 2006;24:754-8.
15. Bosatra M, Jucci A, Olliaro P, et al. In vitro fibroblast and dermis fibroblast activation by laser irradiation at low energy. An electron microscopic study. Dermatologica 1984;168:157-62.
16. Zare F, Moradi A, Fallahnezhad S, et al. Photobiomodulation with 630 plus 810 nm wavelengths induce more in vitro cell viability of human adipose stem cells than human bone marrow-derived stem cells. J Photochem Photobiol B 2019;201:111658.
17. Wang Y, Huang YY, Wang Y, et al. Red (660 nm) or near-infrared (810 nm) photobiomodulation stimulates, while blue (415 nm), green (540 nm) light inhibits proliferation in human adipose-derived stem cells. Sci Rep 2017;7:7781.
18. Li W, Hu X, Lu X, et al. RNA-Seq analysis revealed the molecular mechanisms of photobiomodulation effect on human fibroblasts. Photodermatol Photoimmunol Photomed 2020;36:299-307.
19. de Farias Gabriel A, Wagner VP, Correa C, et al. Photobiomodulation therapy modulates epigenetic events and NF-κB expression in oral epithelial wound healing. Lasers Med Sci 2019;34:1465-72.
20. Weiss RA, McDaniel DH, Geronemus RG, et al. Clinical experience with light-emitting diode (LED) photomodulation. Dermatol Surg 2005;31:1199-205.
21. Tomazoni SS, Costa LOP, Joensen J, et al. Effects of photobiomodulation therapy on inflammatory mediators in patients with chronic non-specific low back pain: Protocol for a randomized placebo-controlled trial. Medicine (Baltimore) 2019;98:e15177.
22. Langella LG, Casalechi HL, Tomazoni SS, et al. Photobiomodulation therapy (PBMT) on acute pain and inflammation in patients who underwent total hip arthroplasty-a randomized, triple-blind, placebo-controlled clinical trial. Lasers Med Sci 2018;33:1933-40.
23. Liu T, Deng Z, Xie H, et al. ADAMDEC1 promotes skin inflammation in rosacea via modulating the polarization of M1 macrophages. Biochem Biophys Res Commun 2020;521:64-71.
24. Yuan X, Li J, Li Y, et al. Artemisinin, a potential option to inhibit inflammation and angiogenesis in rosacea. Biomed Pharmacother 2019;117:109181.
25. Kan HL, Wang CC, Cheng YH, et al. Cinnamtannin

B1 attenuates rosacea-like signs via inhibition of pro-inflammatory cytokine production and down-regulation of the MAPK pathway. PeerJ 2020;8:e10548.
26. Li J, Yuan X, Tang Y, et al. Hydroxychloroquine is a novel therapeutic approach for rosacea. Int Immunopharmacol 2020;79:106178.
27. Lee J, Jung Y, Jeong SW, et al. Inhibition of Hippo Signaling Improves Skin Lesions in a Rosacea-Like Mouse Model. Int J Mol Sci 2021;22:931.
28. Lee JB, Bae SH, Moon KR, et al. Light-emitting diodes downregulate cathelicidin, kallikrein and toll-like receptor 2 expressions in keratinocytes and rosacea-like mouse skin. Exp Dermatol 2016;25:956-61.
29. Kim M, Kim J, Jeong SW, et al. Long-pulsed 1064-nm Nd: YAG laser ameliorates LL-37-induced rosacea-like skin lesions through promoting collagen remodeling in BALB/c mice. Lasers Med Sci 2018;33:393-7.
30. Kim M, Kim KE, Jung HY, et al. Recombinant erythroid differentiation regulator 1 inhibits both inflammation and angiogenesis in a mouse model of rosacea. Exp Dermatol 2015;24:680-5.
31. Chen M, Xie H, Chen Z, et al. Thalidomide ameliorates rosacea-like skin inflammation and suppresses NF-κB activation in keratinocytes. Biomed Pharmacother 2019;116:109011.
32. Li Y, Xie H, Deng Z, et al. Tranexamic acid ameliorates rosacea symptoms through regulating immune response and angiogenesis. Int Immunopharmacol 2019;67:326-34.
33. Korn T, Muschaweckh A. Stability and Maintenance of Foxp3+ Treg Cells in Non-lymphoid Microenvironments. Front Immunol 2019;10:2634.
34. Wang L, Wang YJ, Hao D, et al. Long non-coding RNA NEAT1 functions as a competing endogenous RNA to regulate S100A9 expression by sponging miR-196a-5p in rosacea. J Dermatol Sci 2021;102:58-67.
35. Riedlinger T, Liefke R, Meier-Soelch J, et al. NF-κB p65 dimerization and DNA-binding is important for inflammatory gene expression. FASEB J 2019;33:4188-202.
36. Wang S, Song R, Wang Z, et al. S100A8/A9 in Inflammation. Front Immunol 2018;9:1298.
37. Lakschevitz FS, Hassanpour S, Rubin A, et al. Identification of neutrophil surface marker changes in health and inflammation using high-throughput screening flow cytometry. Exp Cell Res 2016;342:200-9.
38. Morath A, Schamel WW. αβ and γδ T cell receptors: Similar but different. J Leukoc Biol 2020;107:1045-55.
39. Lifshitz L, Tabak G, Gassmann M, et al. Macrophages as novel target cells for erythropoietin. Haematologica 2010;95:1823-31.

(English Language Editor: J. Teoh)

Cite this article as: Wu S, Su Y, Wang L, Sun B, Jiang X. The effects of photobiomodulation therapy on inflammatory mediators, immune infiltration, and angiogenesis in a mouse model of rosacea. Ann Transl Med 2022;10(15):831. doi: 10.21037/atm-22-3204

